15 June 1997

ELSEVIER

Optics Communications 139 (1997) 92–98

OPTICS COMMUNICATIONS

Full length article

Polarised light induced birefringence in azo dye doped polymer: a new model and polarised holographic experiments

P.-A. Blanche [a], Ph.C. Lemaire [a], C. Maertens [b], P. Dubois [b], R. Jérôme [b]

[a] *Centre Spatial de Liège (C.S.L.), Université de Liège, Parc Scientifique du Sart Tilman, Avenue du Pré-Aily, B 4031 Angleur-Liège, Belgium*

[b] *Center for Education and Research on Macromolecules (C.E.R.M.), Université de Liège, Sart Tilmant B6, B 4000 Liège, Belgium*

Received 9 September 1996; revised 3 December 1996; accepted 4 December 1996

Abstract

The photoinduced birefringence of azo dye DMNPAA (2,5-dimethyl-4-(p-nitrophenylazo)anisole) in PVK (poly(N-vinylcarbazole)) thin film is reported. A two-layer model of the film is proposed to take into account the different results obtained in photoinduced birefringence experiments. According to this model, the sample exhibits intrinsic birefringence but the absorbed light can induce orientation of the optically active molecules contained in the first layer of the film, leading to photoinduced birefringence. Holographic experiments have been carried out in this media with recording at 514 nm and readout at 633 nm. Diffraction efficiency versus polarisation shows that these polymers can record polarisation states as well as intensity patterns.

1. Introduction

The ability of some organic materials to become birefringent when illuminated by polarised light has been known for a long time. Some of them have already been studied for polarisation holographic applications [1–5]. In the last few years, many authors have studied both optical and field poling of azo dye in thin polymeric films because of their potential applications to integrated optics [6–9].

In parallel, a great interest has been brought on photorefractive polymers that have many potential applications too. It is generally admitted that the types of recording process are totally different for these two media. The role of cis-trans photoisomerization in the birefringent process has been pointed out [10–12], whereas the space-charge grating formation and the electro-optical effect are necessary to the photorefractivity [13,14].

Recently, a first analogy has been found between both types of recording process: the grating enhancement by orientation of the electro-optical molecules in the photorefractive space charge field [15].

In this paper, we present a type of azo-dye doped polymer, well known for his photorefractive properties [16,17], that shows photoinduced birefringence. This allows us to suppose that the two recording processes are present in photorefractive experiments.

Our sample is constituted by a polymer matrix of PVK (Poly(N-vinylecarbazole)), doped with 10 weight percents (wt %) of the optically active molecule DMNPAA (2,5-dimethyl-4-(p-nitrophenylazo)anisole) (inset in Fig. 1) and 30 wt % of ECZ (N-ethylcarbazole) which acts as a plasticizer. Section 2 will describe the sample preparation and the experimental set-up.

It is accepted that the photoinduced birefringence is due to the orientation of the optically active molecules perpendicularly to the electrical field of polarised light [10–12]. Without illumination, these molecules are randomly turned. That leads to a simple model which does not agree with the experimental results we have obtained. In reply, we propose a new theoretical model developed in Section 3.

In Section 4, we have performed experiments showing that the polymer acts as a polarisation holographic media which is self-developing and re-usable. The figures of merit of our samples in terms of recording medium are

PII S0030-4018(96)00773-0

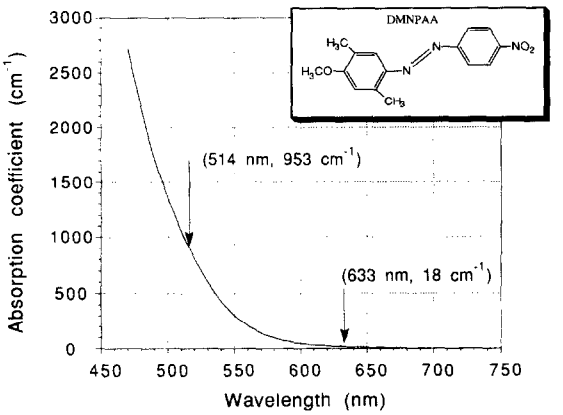

Fig. 1. Absorption coefficient spectrum of a 10 wt % DMNPAA doped PVK film with 30 wt % of ECZ. The absorption coefficient of the two wavelengths used for the experiments presented are indicated. Inset: DMNPAA molecule representation.

quite low but the aim of these experiments was to study the writing process, not to develop a good recording medium.

2. Experiments

2.1. Products

2,5-dimethylphenol (purchased in Janssen), potassium nitrite (Janssen), iodomethane (Aldrich), N-vinylcarbazole (Fluka), p-nitro aniline (Janssen) were used as received. N-ethylcarbazole (Janssen) was purified by two successive recrystallizations from methanol.

2,5-dimethyl-4-(p-nitrophenylazo) anisole (DMNPAA) was synthesised by an azo coupling of 2,5 dimethylphenol with p-nitroaniline followed by Williamson alkylation with iodomethane. Overall yield was 90%. Experimental procedures will be described elsewhere.

The structure was confirmed by ^{1}H nuclear magnetic resonance and Fourier transform infra-red spectroscopy. The purity was checked by thin-layer chromatography.

Poly(N-vinylcarbazole) was synthesised by radical polymerisation of N-vinylcarbazole monomer, initiated by azobis-isobutyronitrile (AIBN), followed by two precipitations in methanol.

2.2. Samples preparation

A 10% in weight blend of DMNPAA in PVK/ECZ matrix (66/33 wt % respectively) was prepared by dissolving the polymer and the doping molecules in tetrahydrofuran (THF). The solution was filtered through a 0.5 μm filter and solvent was further evaporated under reduced pressure in rotavapor (15 mm Hg). The resulting polymer was frozen in liquid nitrogen and crushed in fine powder. Glass temperature (T_g), determined by Differential Scanning Calorimetry (DSC) was found to be around 10°C. This powder is placed on a glass plate between teflon spacers, and heated at 140°C where the polymer begins to flow. A second glass plate is deposited above the other and pressed for 30 minutes to spread out the polymer. This operation provides a film with a good optical quality: homogeneous phase and coloration and without bubbles. By this way, we are able to make films with uniform thickness ranged between 10 and 100 μm depending on the spacer thickness.

The absorption coefficient spectrum of the polymer film recorded between 470 nm and 750 nm is shown in Fig. 1, this result is similar to those presented in Ref. [17].

2.3. Natural and photo-induced birefringence

We have used a 100 μm thickness sample. The natural birefringence of the polymer film has been brought in evidence by placing it between crossed polarisers and by illuminating it by natural light. These experiments have shown that the natural birefringence axes and the phase retardation depend on the location on the film. The natural birefringence is probably a result of the sample preparation since it appeared, in some samples, a correlation between the polarisation axes and the spreading of the polymer during the press process. No means to avoid natural birefringence has been found.

For photo-induced birefringence experiments, two nearly parallel beams are incident to the sample, as shown in Fig. 2. The first one, coming from an argon laser

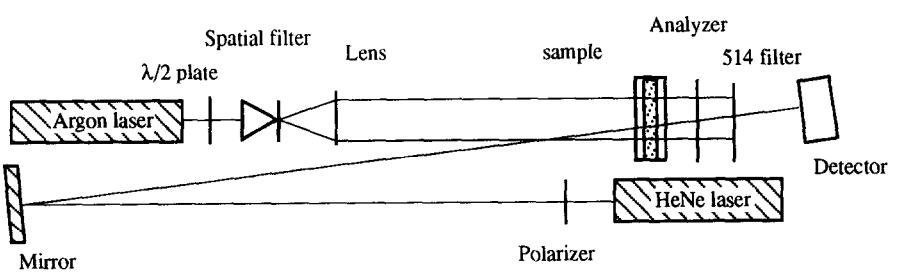

Fig. 2. Geometry of the experimental set-up used for the photoinduced birefringence experiments.

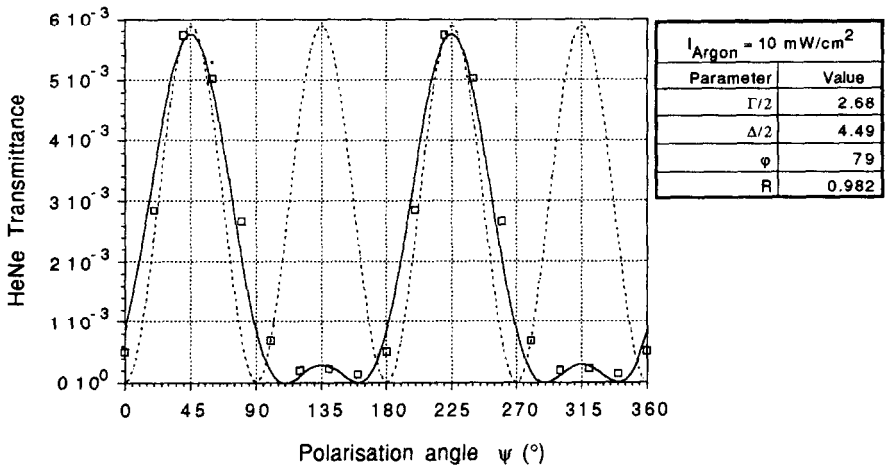

Fig. 3. Transmittance of the HeNe beam versus the polarisation angle between the argon and the HeNe beams. The solid line represents the fit by our two-layer model (Eq. (3)), the parameters are given besides the graph. The dotted curve is the fit by the model taking only into account the photoinduced birefringence (one-layer model: $\Delta = 0$). In order to reach the same transmittance at 45°, the parameter $\Gamma/2$ has been set equal to 4.4.

emitting at a wavelength of 514 nm, is linearly polarised and a half-wave plate is used to rotate the polarisation axis into the proper direction. After being filtered and expanded, this beam reaches the sample where it is strongly absorbed. The second one, a HeNe beam at a wavelength of 633 nm, is also linearly polarised; it traverses the sample where it is weakly absorbed and further, crosses an analyzer rotated at 90° with respect to the incident polarisation. A filter that has an absorption bandwidth centred on 514 nm is placed before the detector in order to stop any diffuse or direct light coming from the argon laser.

This set-up allows us to perform the following measurements. First, by rotating the half-wave plate on the path of the argon beam, we have recorded the transmitted intensity of the HeNe beam versus the angle between the red (fixed) and green beam polarisations. A typical result is shown in Fig. 3. Second, we have monitored the transmitted HeNe light in function of the argon intensity arriving on the sample (Fig. 4).

According to the location where the HeNe beam crosses the sample, the results obtained can change significantly: the curve of the transmitted HeNe intensity as a function

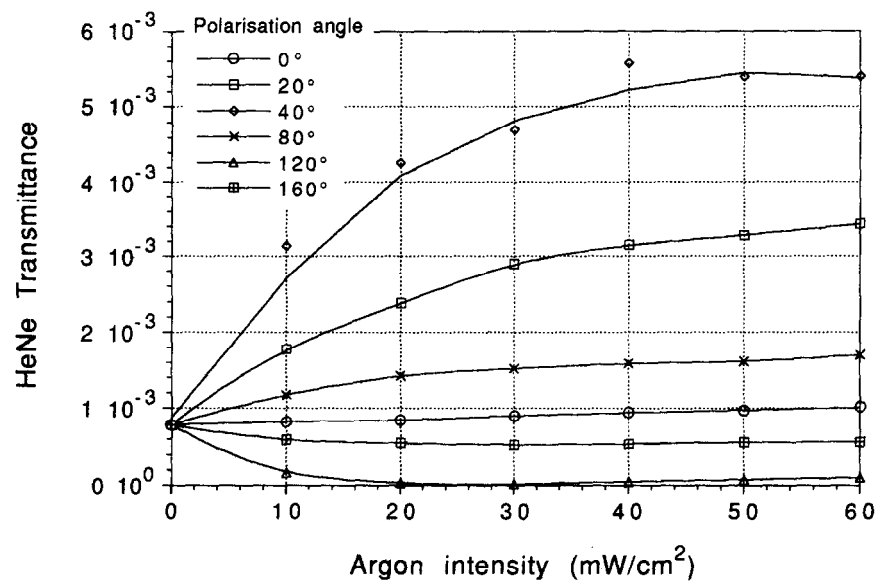

Fig. 4. Transmittance of the HeNe beam versus the intensity of the argon beam for different angles between the polarisation of the beams. The lines have no mathematical meaning, they are only guides to the eyes.

of the angle between the argon and the HeNe light polarisation (Fig. 3) presents four maxima with variable amplitudes for a 360° rotation. In order to take these results into account, we will introduce in the next section a new model describing the polymer behaviour.

3. Model

A model that takes only the photoinduced birefringence into account does not explain the results of transmittance versus the polarisation angle that we have obtained. Indeed, it predicts an equivalent transmission maximum at 45° and 135° whereas it is not the case as seen in Fig. 3. For this reason we have worked out a new simple two-layer model to describe the polymer behaviour. A realistic physical model would probably require an infinite number of layers, each acting as a retardation plate. But, conversely in liquid crystal media, it is not possible to find a relation between the angle of the birefringence axes and the position of the layer. Thus the matrix system does not reduce itself and contains an infinite number of matrices. Moreover, in view of the results obtained by the two-layer model, it seems not useful to complicate the system by increasing the number of layers.

In our model, the sample acts as two birefringent plates. The first one is able to orientate its principal axis on the direction of the incident argon light polarisation and its thickness (or its effective phase retardation) depends on the beam power. This layer absorbs the major part of the beam; indeed, for a 514 nm beam at 60 mW/cm^2 (the maximum of intensity used in our experiments), we find only 1 mW/cm^2 at 43 μm depth (at this intensity, effects are negligible: see Fig. 4). Thus only an insignificant intensity reaches the second layer. At this location, the intensity is too weak to generate light induced birefringence. However, the second layer has a natural birefringence and its principal axis, as well as its phase retardation, depend on the location in the material. The representation of such a system is shown in Fig. 5.

One can represent the transmission of this optical system, placed in front of an analyzer, by a product of Jones matrices, giving

$$E' = \begin{pmatrix} 1 & 0 \\ 0 & 0 \end{pmatrix} R(-\varphi) \begin{pmatrix} e^{-i\Delta/2} & 0 \\ 0 & e^{i\Delta/2} \end{pmatrix} R(\varphi) R(-\psi) \times \begin{pmatrix} e^{-i\Gamma/2} & 0 \\ 0 & e^{i\Gamma/2} \end{pmatrix} R(\psi) \begin{pmatrix} 0 \\ 1 \end{pmatrix}, \quad (1)$$

where the rotation matrices $R(\theta)$ are defined as follows:

$$R(\theta) = \begin{pmatrix} \cos(\theta) & \sin(\theta) \\ -\sin(\theta) & \cos(\theta) \end{pmatrix}. \quad (2)$$

Eq. (1) means that the HeNe light, polarised along to the x axis, crosses the first birefringent layer (photoinduced) whose axis is orientated by a ψ angle with respect to x and induces a phase retardation of Γ. The light is further transmitted through the second birefringent layer (natural one), whose axis is rotated by an angle φ with respect to the x axis and has a phase retardation Δ. At the end of the optical system, an analyzer, crossed with respect to x, filters the output polarisation.

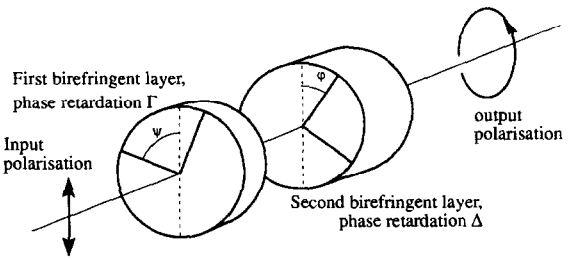

Fig. 5. Equivalent optical system of the polymer film (argon beam is not shown). The beam traversing the system comes from the HeNe laser. The first birefringent layer has its principal axis turned in the argon beam polarisation direction, its phase retardation depends on the argon beam intensity. The second birefringent layer is self-orientated because the argon light does not penetrate into this layer: it has been absorbed by the first layer.

The transmitted intensity can be expressed by the development of the matrix equation (1):

$$\begin{aligned} I_{\text{transmitted}} &= E'E'^{*} \\ &= \sin^2(\Gamma/2)\sin^2(2\psi) \\ &\quad \times \left(\cos^2(\Delta/2) + \sin^2(\Delta/2)\cos(2\varphi)\right) \\ &\quad + \sin^2(\Delta/2)\sin^2(2\varphi) \\ &\quad \times \left(\cos^2(\Gamma/2) + \sin^2(\Gamma/2)\cos(2\psi)\right) \\ &\quad + \tfrac{1}{2}\left(\sin(\Delta)\sin(\Gamma)\sin(2\psi)\sin(2\varphi)\right. \\ &\quad \left. + \sin^2(\Gamma/2)\sin^2(\Delta/2)\sin(4\psi)\sin(4\varphi)\right). \end{aligned} \quad (3)$$

For a one-layer model, $\Delta = 0$ since there is no natural birefringence.

At this step we have a model with three unknown parameters (Δ, Γ, φ) which can be determined by the fit of the theoretical function (3) to the experimental measurements of the transmitted intensity in function of the angle ψ (Fig. 3). This latter one is equal to the angle between the polarisation of the argon beam and the polarisation of the HeNe beam.

4. Results and discussion

4.1. Optically induced molecular orientation

The result of such a fit is presented in Fig. 3 (solid line). As it can be seen, our model is in good agreement

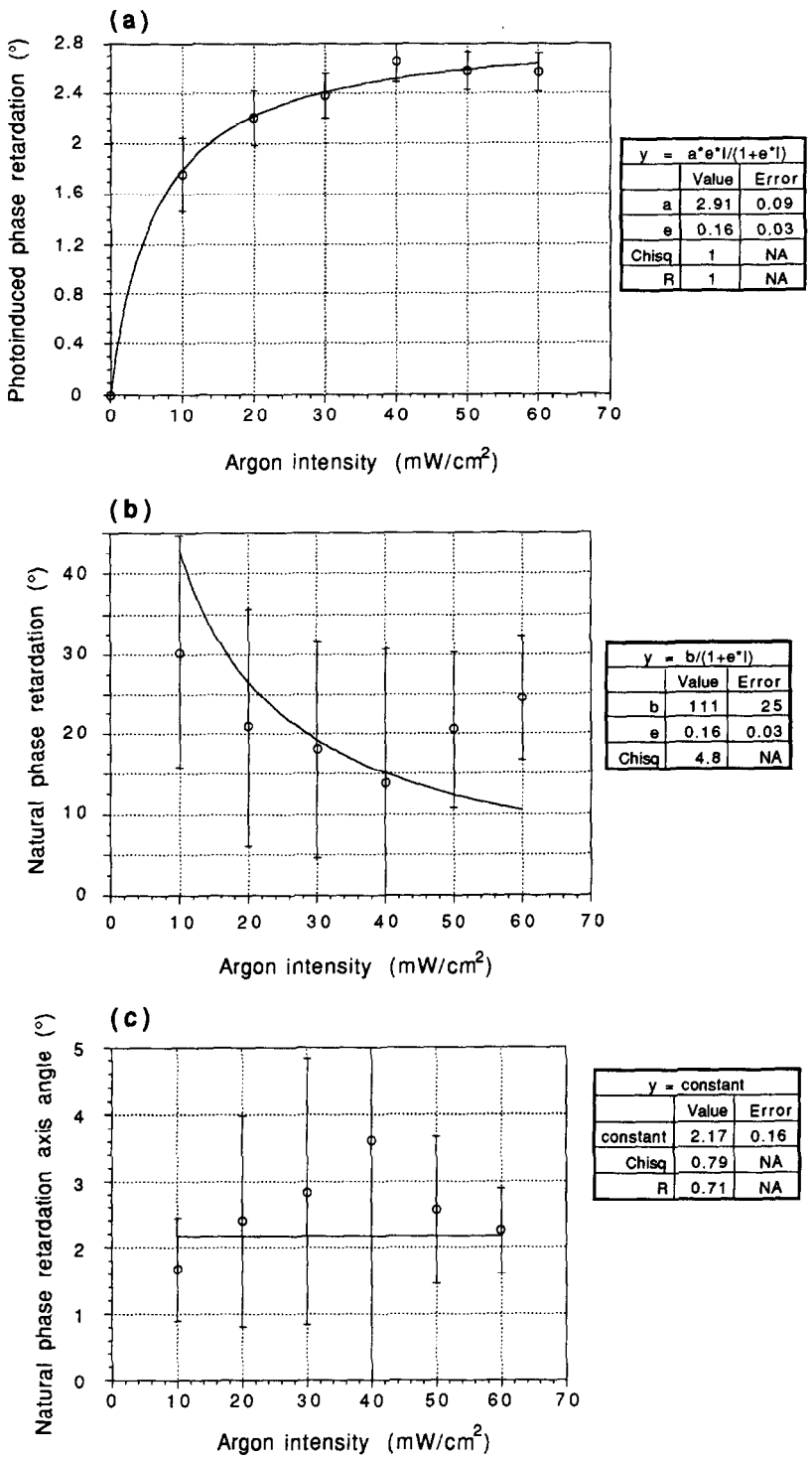

Fig. 6. The plots obtained by fitting in the photoinduced birefringence experiments versus the argon polarisation angle, we obtain a triplet of parameters: Γ, Δ, φ. The figures show the plot of these parameters versus the argon intensity for an argon polarisation angle fixed at 40° according to the HeNe polarisation axis. In the three cases, the curve fit is deduced from our model. Inset: fit function and parameter values. (a) Photoinduced phase retardation Γ versus argon intensity. (b) Natural phase retardation Δ versus argon intensity. (c) Axis angle φ of the natural birefringence versus argon intensity.

with the measurement, contrary to a one-layer model (dotted line) which predicts the same transmission maximum at 45° and 135°.

Fig. 6 shows the different parameters (Δ, Γ, φ) as a function of the poling beam intensity. These values result from the above mentioned procedure of fitting (least squares). The error bars are the standard errors on the parameters given by the fit program. As expected, the induced phase retardation Γ increases with the intensity of the poling beam. The higher the poling intensity, the higher the number of molecules that are aligned by the beam polarisation. We observe also a saturation when all molecules are aligned. The behaviour of Γ can be described by the following phenomenological equation,

$$\Gamma = aeI/(1 + eI), \tag{4}$$

where a is the maximum photoinduced phase retardation, e the efficiency with which the light induces phase retardation and I the intensity of the argon beam (see Fig. 6a).

Conversely, Δ, representing the natural birefringence, is maximum when there is no illumination and decreases according to the power of the argon beam. Indeed, when we increase the poling intensity, the photoinduced birefringence stands in for the natural one. The latter decreases to zero when all the molecules are aligned by the laser, so Δ can be expressed by the following equation, where b is the phase retardation of the sample without illumination (see Fig. 6b):

$$\Delta = b/(1 + eI). \tag{5}$$

The last variable, φ, is a constant if the HeNe beam does not change location in the sample during the experiments (Fig. 6c).

Once again, these models are in relatively good agreement with the measurement.

4.2. Polarisation holography

The preceding experiments have proved that the polymer can record the polarisation state of the argon beam. We have used this property to write polarisation holograms in the sample. The linearly polarised argon beam is split into two parts, one polarisation is rotated by 90°, and these orthogonal polarised beams cross themselves into the sample. In such a situation the beams do not interfere in intensity, however a similar pattern information is created by means of the polarisation state which is modulated consequently to the optical path difference [18]. A non-polarised HeNe beam is used to read out the hologram at the Bragg angle.

By using a total recording power of 2×20 mW/cm^2 (beam ratio 1/1, linear polarisation orthogonal to each other), we have obtained a diffraction efficiency of the HeNe beam of about 0.02% and a sensitivity $S_{\eta 1} = (\mathrm{d}\eta/\mathrm{d}w)(1/d) = 0.1$ (J/cm^2)$^{-1}$. The fact that we can write a hologram in such a polarisation configuration proves that the media can record the polarisation state. In this kind of experiment, the photorefractive recording process can be dismissed because, by its nature, this process can only record an intensity grating. The dynamic of recording and erasing can be seen in Fig. 7. Further experiments on holographic recording are currently being done to improve our knowledge on this material.

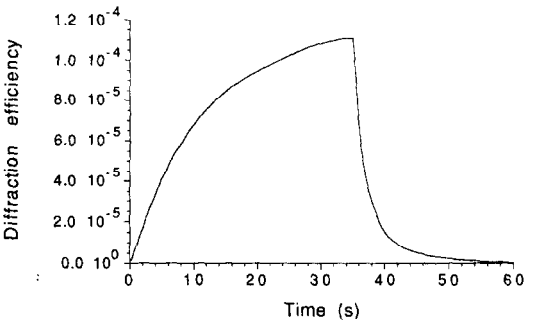

Fig. 7. Diffraction efficiency versus time on a 100 μm thick film. The argon beams are switched on at $t = 0$ and one of them is switched off at $t = 35$ s. Total argon intensity is 40 mW/cm^2, beam ratio is 1/1, linear polarisation orthogonal to each other.

5. Conclusions

We have shown that a non-linear molecule used in a photorefractive polymer shows photoinduced birefringence in response to polarised light. This material can be used as a polarised recording medium. This supposes that the electro-optical and photo-orientation effects are certainly acting in photorefractive experiments using these molecules.

We have introduced a new model describing the polymer film behaviour in the photoinduced birefringent experiment. This model separates the sample into two layers, the first one strongly absorbs the polarised argon light inducing an orientation of the molecules in the beam polarisation. This leads to a photoinduced birefringence whose phase retardation depends on the beam intensity. The argon light does not penetrate into the second layer which only presents natural birefringence affecting the polarisation too.

Using the principle of polarisation holography recording, we have carried out diffraction experiments to prove the nature of the recording process and for determining the figure of merit of the polymer film. The maximum diffraction efficiency that could be achieved by writing with orthogonal polarised beams is 0.02%, and the sensitivity is $S_{\eta 1} = (\mathrm{d}\eta/\mathrm{d}w)(1/d) = 0.1$ (J/cm^2)$^{-1}$ depending on the experimental conditions. We are presently studying new

side-chain polymers in order to improve the figures of merit of the polymer films.

References

[1] T. Todorov, L. Nokolova and N. Tomova, Appl. Optics 23 (1984) 4309.
[2] S. Calixto and R.A. Lessard, Appl. Optics 23 (1984) 4313.
[3] M.S. Ho, A. Natansohn and P. Rochon, Macromolecules 28 (1995) 6124.
[4] E. Mohajerani, E. Whale and G.R. Mitchell, Optics Comm. 92 (1992) 403.
[5] S.V. O'Leary, Optics Comm. 104 (1994) 245.
[6] Z. Sekkat and M. Dumont, Appl. Phys. B 54 (1992) 486.
[7] L. Läsker, T. Fischer, J. Stumpe, S. Kostromin, S. Ivanov, V. Shibaev and R. Ruhmann, Mol. Cryst. Liq. Cryst. 246 (1994) 347.
[8] D.J.O. Orzi and J.O. Tocho, Opt. Eng. 35 (1996) 47.
[9] T. Huang and K.H. Wagner, J. Opt. Soc. Am. B 13 (1996).
[10] G.S. Kumar and D.C. Neckers, Chem. Rev. 89 (1989) 1915.
[11] Z. Sekkat, D. Morichère, M. Dumont, R. Loucif-Saïbi and J.A. Delaire, J. Appl. Phys. 71 (1992) 1543.
[12] T. Sasaki, T. Ikeda and K. Ichimura, Macromolecules 26 (1993) 151.
[13] L. Yu, W.K. Chan, Z. Peng and A. Gharavi, Acc. Chem. Res. 29 (1996) 13.
[14] H.J. Bolink, V.V. Krasnikov, G.G. Malliaras and G. Hadzioannou, Advanced Materials 6 (1994).
[15] W.E. Moerner, S.M. Silence, F. Hache and G.C. Bjorklund, J. Opt. Soc. Am. B 11 (1994).
[16] B. Kippelen, N. Peyghambarian, S.R. Lyon, A.B. Padias and H.K. Hall Jr, Electron. Lett. 29 (1993).
[17] B.L. Volodin, Sandalphon, K. Meerholz, B. Kippelen, N.V. Kukhtarev and N. Peyghambarian, Opt. Eng. 34 (1995) 2213.
[18] T. Huang and K.H. Wagner, J. Opt. Soc. Am. B 13 (1996) 282.